Scientific Foundation SPIROSKI, Skopje, Republic of Macedonia
Open Access Macedonian Journal of Medical Sciences. 2020 Dec 25; 8(T1):627-633.
https://doi.org/10.3889/oamjms.2020.5631
eISSN: 1857-9655
Category: *T1 - Thematic Issue "Coronavirus Disease (COVID-19)"*
Section: *Radiology and Radiotherapy*

Findings of Serial Computed Tomography Imaging in Patients with Coronavirus Disease-19

Masoomeh Raoufi[1], Shahram Kahkouee[2], Jamileh Bahri[1], Neda Khalili[3,4], Farzaneh Robatjazi[1], Nastaran Khalili[3,4]*

[1]Department of Radiology, School of Medicine, Imam Hossein Hospital, Shahid Beheshti University of Medical Sciences, Tehran, Iran; [2]National Research Institute of Tuberculosis and Lung Diseases, Shahid Beheshti University of Medical Sciences, Tehran, Iran; [3]School of Medicine, Tehran University of Medical Sciences, Tehran, Iran; [4]Network of Immunity In Infection, Malignancy and Autoimmunity, Universal Scientific Education and Research Network, Tehran, Iran

Edited by: Branislav Filipović
Citation: Raoufi M, Kahkouee S, Bahri J, Khalili N, Robatjazi F, Khalili N. Findings of Serial Computed Tomography Imaging in Patients with Coronavirus Disease-19. Open Access Maced J Med Sci. 2020 Dec 25; 8(T1):627-633. https://doi.org/10.3889/oamjms.2020. 5631
Keywords: Coronavirus Disease-2019; Computed Tomography; Organizing Pneumonia; Serial Imaging
***Correspondence:** Nastaran Khalili, School of Medicine, Tehran University of Medical Sciences, Tehran, Iran. E-mail: nkhalili71@gmail.com
Received: 24-Aug-2020
Revised: 12-Dec-2020
Accepted: 22-Dec-2020

Funding: Publication of this article was financially supported by the Scientific Foundation SPIROSKI, Skopje, Republic of Macedonia
Competing Interests: The authors have declared that no competing interests exist

Abstract

AIM: We investigated the serial changes of chest computed tomography (CT) in patients with coronavirus disease-2019 (COVID-19) presenting with viral-induced lung damage on follow-up CT.

METHODS: We evaluated 66 patients with confirmed COVID-19, who had undergone at least two chest CTs from February 24 to April 21, 2020. Nine patients also had a third CT. All patients demonstrated viral-induced lung damage (organizing pneumonia-like pattern) on second CT. The involvement pattern of each lobe and the extent of infiltration (based on CT score) were assessed on serial CTs to determine changes throughout the disease course. Patients' demographic and clinical data and final outcome were also recorded.

RESULTS: Mean age (standard deviation [SD]) of patients was 56.04 (15.2) years old; 51.5% were male. About 93.9% of patients had survived. Mean (SD) interval between the first and second CT and second and third CT was 7.6 (5.9) and 16.8 (8.3) days, respectively. The extent of total lung involvement was significantly higher in the second CT compared with the first CT ($p < 0.001$) and also increased non-significantly in the third CT ($p = 0.29$). The right lower lobe persistently had the highest CT score through the disease course.

CONCLUSION: Evaluation of serial CT imaging can reveal information regarding the stage of COVID-19, thus providing help for appropriate treatment planning.

Introduction

The diagnosis of coronavirus (CoV) disease-2019 (COVID-19) is confirmed through real-time reverse transcriptase-polymerase chain reaction assay (RT-PCR) of upper respiratory tract specimens [1], but imaging modalities have also proved to be helpful for the diagnosis of COVID-19. In particular, computed tomography (CT) imaging is capable of monitoring disease progression and clinical response in COVID-19 [2], [3].

It is currently evident that COVID-19 is mainly associated with respiratory distress and acute lung injury; however, the long-term sequelae of COVID-19 on the lung parenchyma and pulmonary function are not yet clear. A study on patients recovered from nosocomial severe acute respiratory syndrome (SARS) infection showed that even after 15 years of follow-up, chest CT abnormalities were not completely resolved, and residual lesions still existed on imaging [4]. Organizing pneumonia (OP) is a radio-histologic pattern commonly formed subsequent to lung damage in patients with focal or diffuse lung injury [5]. Many etiologies contribute to the secondary OP, among them, viral pneumonia such as H1N1 influenza, SARS-CoV, and Middle East respiratory syndrome-CoV [6], [7], [8]. Several studies have already reported the presence of viral-induced lung damage (OP-like pattern) in patients infected with SARS-CoV-2 [9], [10]. A diverse range of clinical outcomes is observed in patients with viral-induced lung damage (OP-like pattern), ranging from complete resolution of lesions to more severe progressive consequences such as pulmonary fibrosis [11], [12]. Hence, in patients who have developed viral-induced lung damage (OP-like pattern), CT is useful for determining the outcomes of lung involvement and defining patients' long-term prognosis. Herein, we aimed to evaluate serial changes of CT imaging in hospitalized patients with confirmed COVID-19 who had manifested with viral-induced lung damage (OP-like pattern) on their second CT scan.

Materials and Methods

Study design and participants

In this retrospective study, we evaluated 66 adult patients (age >18 years old) with a laboratory-confirmed diagnosis of COVID-19, who were hospitalized in our referral hospital from February 24 to April 21, 2020, and had underwent at least two CT scans. All of the enrolled patients had imaging findings consistent with viral-induced lung damage (OP-like pattern) on their second CT scan. COVID-19 diagnosis was confirmed with positive RT-PCR assay for SARS-CoV-2 obtained from a nasopharyngeal swab specimen and diagnosis of viral-induced lung damage (OP-like pattern) was based on consistent imaging findings on CT.

All patients underwent the second CT scan due to clinical indication. In nine patients, a third CT scan had also been performed. According to national COVID-19 guidelines, non-contrast low-dose CT was performed for all patients with reconstructions of the volume at 3 mm–5 mm slice thickness. CT images were reviewed by two board-certified radiologists with 4 and 10 years of experience. Both radiologists were blinded to the lab data, clinical features, and patients' diagnosis. Imaging findings were first interpreted independently and in case of disagreement, final decision was reached by consensus. For reporting imaging features, international standard nomenclature defined by the Fleischner Society was used [13]. The involvement pattern of each specific lobe on the first, second, and third CT was recorded to determine serial changes of imaging. Furthermore, the extent of lobar involvement was assessed using a scoring system as follows: a numerical score was assigned to each of the five lobes based on the percentage of infiltration in each lobe: 0 (none), 1 (1–5%), 2 (6–25%), 3 (26–49%), 4 (50–75%), and 5 (>75%); total score was obtained by summing the scores of all lobes for each patient. In addition to imaging findings, patients' demographic and clinical data and final disease outcome were also collected.

Statistical analysis

Categorical variables are reported as number (percentages) and continuous variables are expressed as mean (standard deviation [SD]) and range. Normality tests were used to assess distribution. Continuous data were compared between the groups using t-test and categorical variables were compared using Chi-square or Fisher's exact test. Statistical tests were performed by SPSS v.23 (IBM Inc., Chicago, IL, USA). $p < 0.05$ was considered statistically significant.

Ethics approval

This study was approved by the ethical review board of our institution (Ethics code: IR.SBMU.MSP.REC.1399.084) and Helsinki Declaration of 1975, as revised in 2000. Written informed consent was waived due to retrospective nature of study.

Results

Table 1 presents patients' demographic and clinical data. The mean age (SD) of patients was 56.04 (15.2) years old; 51.5% were male. The most common clinical manifestation was respiratory distress (93.9%) followed by fever (45.4%). The mean (SD) interval from symptom onset to presentation was 7.50 (4.11) days and the median hospitalization time was 5 days; however, this duration varied from 1 to 34 days. Considering patients' final outcome, 93.9% had survived and six patients had experienced death. Seven patients (10.6%) had leukocytopenia (leukocyte <4 × 10^9/L) and elevated CRP level (>50 mg/dL) was observed in 22/66 (33.3%) patients. More than half of patients had co-existing morbidities (51.5%) with hypertension and diabetes being the most prevalent (Table 1).

Table 1: Demographic and clinical data of patients (n = 66)

Variable	Result
Age, years	56.0 (15.2) 23–93
Gender	
Male	34 (51.5)
Female	32 (48.5)
Duration of hospitalization, days	9.65 (7) 1–34
Symptom onset to presentation, days	
0–4	9 (13.6)
4–14	51 (77.3)
>14	6 (9.1)
Outcome	
Ward	54 (81.8)
Intensive care unit	8 (12.1)
Death	4 (6.1)
Lab data	
C-reactive protein (mg/dL)	55.6 (48.4)
Lymphocyte (× 109/L)	1.46 (1.6)
Leukocyte (× 109/ L)	7.29 (6.6)
Comorbidities	
Diabetes	18 (27.2)
Hypertension	23 (34.8)
Hyperlipidemia	9 (13.6)
Ischemic heart disease	6 (9.1)
Chronic kidney disease	2 (3)
Other	2 (3)
Presenting symptoms	
Fever and chills	30 (45.4)
Respiratory distress	61 (93.9)
Neurologic involvement	7 (10.6)
Gastrointestinal involvement	17 (25.7)
Time from first to second CT (days)	7.6 (5.9) 2–30
Time from second to third CT (days)	16.8 (8.3) 7–30

Continuous data are represented as mean (SD) and range. Categorical data are reported as n (%). [a]This includes patients presenting with cough or dyspnea. CT: Computed tomography, CI: Confidence interval, RUL: Right upper lobe, RML: Right middle lobe, RLL: Right lower lobe, LUL: Left upper lobe, LLL: Left lower lobe. SD: Standard deviation

The mean (SD) interval between the first and second CT was 7.6 (5.9) days; this duration was 16.8 (8.3) days for the second and third CT. Table 2 shows the extent of lung involvement in each lobe on first, second, and third CT. As shown, through different time

Table 2: Extent of lung involvement based on CT score

Lobe	First CT score (n = 66)	Second CT score (n = 66)	p-value (95% CI)[a]	Third CT score (n = 9)	p-value (95% CI)[b]
RUL	1.98 (0.92)	2.45 (8.98)	<0.001 (0.26–0.68)	2.33 (1.00)	0.44 (−0.61–1.27)
RML	1.58 (0.95)	2.02 (0.92)	<0.001 (0.23–0.65)	2.44 (1.24)	0.51 (−0.52–0.96)
RLL	2.33 (1.03)	2.89 (0.82)	<0.001 (0.29–0.83)	2.78 (0.83)	0.68 (−0.71–0.49)
LUL	1.94 (1.13)	2.53 (0.95)	<0.001 (0.33–0.84)	2.67 (0.71)	0.28 (−0.99–0.33)
LLL	2.11 (0.99)	2.76 (0.82)	<0.001 (0.40–0.91)	2.56 (1.01)	0.45 (−0.86–0.48)
Total score (range)	9.93 + 3.77 (0–18)	12.65 + 3.07 (4–19)	<0.001 (1.75–3.66)	15.55 + 4.03 (11–22)	0.29 (−1.63–4.75)

Data are reported as mean (SD). [a]p-value (95% CI) represents the statistical difference between first and second CT. [b]p-value (95% CI) represents the statistical difference between second and third CT. CT: Computed tomography, SD: Standard deviation.

points, the right lower lobe was involved at a greater extent compared with other lobes. More importantly, the results of our study showed that the CT score of all lobes was significantly higher in the second CT compared with the first CT. Furthermore, in patients who had undergone a third CT, it was shown that there was a greater amount of lung involvement as compared with the second CT, although not statistically significant.

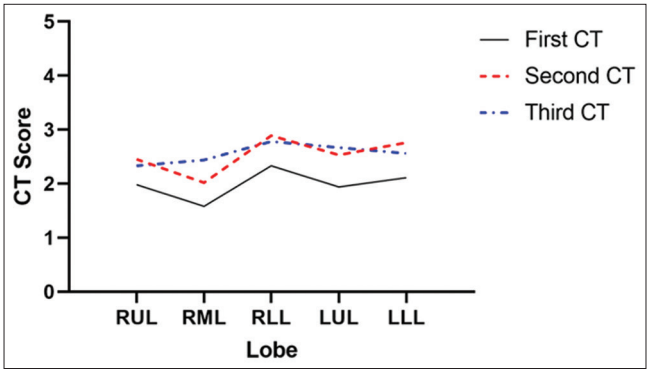

Figure 1: Mean computed tomography (CT) score of each lung lobe on first, second, and third CT

Figure 1 shows the median CT score of each specific lobe on first, second, and third CT scan. Figure 2 shows the total CT score based on the time from admission.

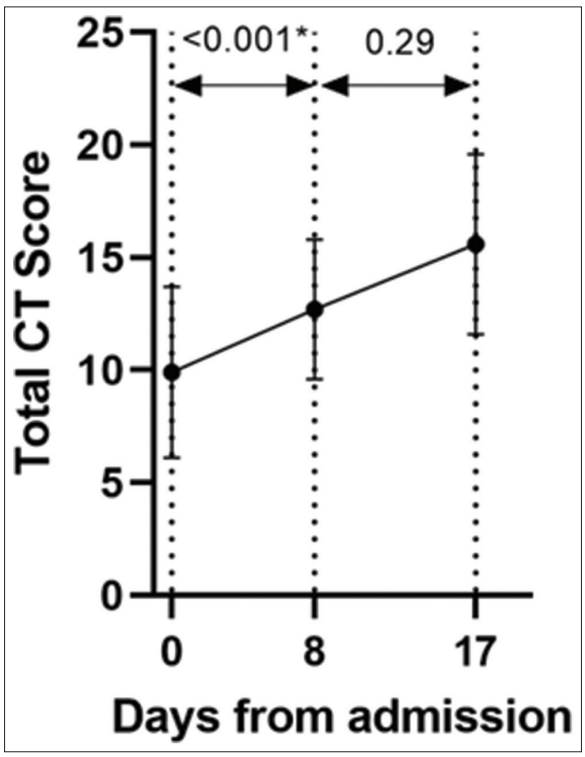

*Figure 2: Serial changes of total computed tomography score after admission (*p-value statistically significant)*

Table 3 shows in detail the serial changes in the involvement pattern of each specific lobe. On the first CT, ground-glass opacity (GGO) was the main involvement pattern in all lobes. The presence of this pattern ranged from 56.1% in the right middle lobe to 75.7% in the right upper lobe. As a show, the pattern of viral-induced lung damage (OP-like pattern) tended to remain in the majority of patients who had third CT. Regarding the changes in lesion distribution, in the first and second CT, peripheral distribution was the most common; however, there was a shift towards a diffuse pattern of involvement in the third CT (Table 4). When comparing the presence of other abnormal findings (Table 5), there was a substantial increase in the number of patients with pleural effusion in the second CT compared with the first (1.5% vs. 19.7%).

Discussion

In this study, we aimed to investigate the changes in serial chest CT imaging of patients with confirmed COVID-19 who, due to clinical indications, underwent a second or third follow-up chest CT during hospitalization and had developed viral-induced lung damage (OP-like pattern) on second CT. In a retrospective observation, we found that the total CT score as well as the CT score of all five lobes was significantly higher in the second CT scans compared with that of the initial CT scans, and also those from the third CT scans were higher, although not significant, than the second CT scans. In both the first and second CT scans, the right lower lobe and left lower lobe had the highest extent of involvement. This is consistent with previous studies that reported a basal predominance of pulmonary lesions among patients with COVID-19 [14], [15]. Furthermore, viral-induced lung damage (OP-like pattern) was most frequently seen in the right and left lower lobes, supporting the previously described predominance of lower lobes in viral-induced lung damage [16].

Viral pulmonary infections can cause a pattern of lung injury that is characterized by fibroblast proliferation. This pattern, which is seen in the organizing phase of diffuse alveolar damage and OP, has both histological and radiological manifestations [17]. Based on the current evidence, COVID-19 infection can similarly result in secondary

Table 3: Serial changes in CT involvement pattern

Lobe	First CT (n = 66)	Second CT (n = 66)	Third CT (n = 9)
RUL			
Primary pattern			
GGO	50 (75.7)	14 (21.2)	2 (22.2)
Consolidation	12 (18.2)	11 (16.7)	1 (11.1)
Crazy-paving	1 (1.5)	4 (6.1)	-
Reversed-halo	1 (1.5)	11 (16.7)	-
Smooth round GGO/consolidation	7 (10.6)	1 (1.5)	-
Non-specific pattern of GGO/consolidation	7 (10.6)	2 (3)	-
Irregular round GGO/consolidation	8 (12.1)	2 (3)	-
Viral-induced lung damage (OP-like pattern)	-	40 (60.6)	6 (66.7)
Sub-pleural band	-	12 (18.2)	1 (11.1)
PBV opacity	-	8 (12.1)	1 (11.1)
Bronchial dilation	-	10 (15.2)	-
Air space nodule	-	4 (6.1)	-
Sub-pleural consolidation	-	1 (1.5)	-
Fibrosing interstitial network	-	3 (4.5)	1 (11.1)
Reticulation	-	-	4 (44.1)
Complete resolution	-	-	1 (11.1)
RML			
Primary pattern			
GGO	44 (66.7)	14 (21.2)	4 (44.4)
Consolidation	12 (18.2)	9 (13.6)	1 (11.1)
Crazy-paving	1 (1.5)	2 (3)	-
Reversed-halo	-	-	-
Smooth round GGO/consolidation	7 (10.6)	-	-
Non-specific pattern of GGO/consolidation	9 (13.6)	5 (7.6)	-
Irregular round GGO/consolidation	5 (7.6)	2 (3)	-
Viral-induced lung damage (OP-like pattern)	-	41 (61.2)	5 (55.5)
Sub-pleural band	-	5 (7.6)	-
PBV opacity	-	5 (7.6)	-
Bronchial dilation	-	19 (28.8)	-
Air space nodule	-	11 (16.7)	1 (11.1)
Sub-pleural consolidation	-	-	-
Fibrosing interstitial network	-	1 (1.5)	1 (11.1)
Reticulation	-	5 (7.6)	3 (33.3)
Complete resolution	-	-	-
RLL			
Primary pattern			
GGO	37 (56.1)	2 (3)	3 (33.3)
Consolidation	22 (33.3)	6 (9.1)	1 (11.1)
Crazy-paving	-	2 (3)	-
Reversed-halo	-	2 (3)	-
Smooth round GGO/consolidation	10 (15.2)	-	-
Non-specific pattern of GGO/consolidation	7 (10.6)	-	-
Irregular round GGO/consolidation	6 (9.1)	-	-
Viral-induced lung damage (OP-like pattern)	-	56 (84.8)	7 (77.7)
Sub-pleural band	1 (1.5)	25 (37.9)	4 (44.4)
PBV opacity	-	9 (13.6)	-
Bronchial dilation	-	17 (25.7)	-
Air space nodule	-	1 (1.5)	-
Sub-pleural consolidation	-	3 (4.5)	1 (11.1)
Fibrosing interstitial network	-	7 (10.6)	1 (11.1)
Reticulation	-	9 (13.6)	9 (100)
Peri-lobular pattern	-	4 (6.1)	-
Complete resolution	-	-	-
LUL			
Primary pattern			
GGO	45 (68.2)	13 (19.7)	3 (33.3)
Consolidation	10 (15.2)	9 (13.6)	1 (11.1)
Crazy-paving	1 (1.5)	2 (3)	-
Reverse-halo	-	2 (3)	-
Smooth round GGO/consolidation	6 (9.1)	-	-
Non-specific GGO/consolidation	11 (16.7)	5 (7.6)	-
Irregular round GGO/consolidation	4 (6.1)	2 (3)	-
Viral-induced lung damage (OP-like pattern)	-	39 (59.1)	-
Sub-pleural band	-	11 (16.7)	6 (66.7)
PBV opacity	-	10 (15.2)	2 (22.2)
Bronchial dilation	-	9 (13.6)	-
Air space nodule	-	3 (4.5)	-
Sub-pleural consolidation	-	2 (3)	-
Fibrosing interstitial network	-	1 (1.5)	-
Reticulation	-	7 (10.6)	-
Peri-lobular pattern	-	-	3 (33.3)
Complete resolution	-	-	-
LLL			
Primary pattern			
GGO	38 (57.6)	1 (1.5)	2 (22.2)
Consolidation	20 (30.3)	6 (9.1)	-
Crazy-paving	1 (1.5)	2 (3)	-
Reversed-halo	-	2 (3)	-
Smooth round GGO/consolidation	7 (10.6)	-	-
Non-specific pattern of GGO/consolidation	11 (16.7)	1 (1.5)	-
Irregular round GGO/consolidation	6 (9.1)	-	-
Viral-induced lung damage (OP-like pattern)	-	57 (86.4)	9 (100)
Sub-pleural band	1 (1.5)	29 (43.9)	5 (55.5)
PBV opacity	-	7 (10.6)	-
Bronchial Dilation	-	10 (15.2)	-
Air space nodule	-	4 (6.1)	2 (22.2)
Sub-pleural consolidation	-	3 (4.5)	1 (11.1)
Fibrosing interstitial network	-	7 (10.6)	1 (11.1)
Reticulation	-	9 (13.6)	2 (22.2)
Peri-lobular pattern	-	1 (1.5)	-
Complete resolution	-	-	-

CT: Computed tomography, GGO: Ground-glass opacity.

Table 4: Serial changes in axial distribution of lung lesions

Lobe	First CT (n = 66)	Second CT (n = 66)	Third CT (n = 9)
RUL			
Diffuse	18 (27.2)	22 (33.4)	5 (55.5)
Peri-bronchovascular	9 (13.6)	8 (12.2)	1 (11.1)
Peripheral	39 (59.1)	36 (54.5)	2 (22.2)
RML			
Diffuse	19 (28.8)	21 (31.8)	5 (55.5)
Peri-bronchovascular	6 (9.1)	7 (10.5)	1 (11.1)
Peripheral	41 (62.1)	38 (57.5)	3 (33.3)
RLL			
Diffuse	18 (27.2)	21 (31.8)	6 (66.7)
Peri-bronchovascular	6 (9.1)	6 (9.1)	-
Peripheral	42 (63.6)	39 (59.1)	3 (33.3)
LUL			
Diffuse	19 (28.8)	23 (34.8)	6 (66.7)
Peri-bronchovascular	7 (10.5)	6 (9.1)	-
Peripheral	40 (60.6)	37 (56.1)	3 (33.3)
LLL			
Diffuse	16 (24.2)	20 (30.3)	6 (66.7)
Peri-bronchovascular	7 (10.5)	5 (7.5)	1 (11.10
Peripheral	43 (65.1)	41 (62.1)	2 (22.2)

Data are reported as n (%).

OP [18], [19], [20]. Although the majority of cases with OP resolve, irreversible fibrosis occurs in some instances [17]. Limited evidence is currently available on the pulmonary sequela and residual radiologic abnormalities in those who have survived. On the other hand, as indicated by studies from previous pandemics, resolution of pulmonary imaging abnormalities may take several months to even several years [4], [21], [22]. In a recently published study by Liu *et al*., the cumulative percentage of complete radiological resolution at 3-weeks post-discharge was 53%. They concluded that COVID-19-associated pulmonary lesions may resolve approximately 2 weeks after discharge. In addition, 3 weeks after discharge, GGO, and fibrous stripe were the most common radiologic findings on CT [23]. Another study investigating the time course of chest CT changes during COVID-19 recovery found that gradual resolution of consolidation occurs ≥14 days after symptom onset. In this stage, also known as the absorption stage, the chest CT scores began to decrease [24]. This is in contrast with our study in that the total CT score of the third CT scan, which was performed approximately 17 days after initial CT, was higher than that of the first and second CT scans. Earlier studies on patients with COVID-19 reported that maximum lung involvement occurs approximately 10 days after the onset of initial symptoms [1], [24]. However, in a case report by Duan and Qin, GGOs in the right and left lower lobes started to resolve at day 7 after admission, while GGOs in the right lower lobe completely resolved at day 13 after admission [25]. These varying findings prompt further follow-up studies in convalescent patients after COVID-19.

Table 5: Serial changes in abnormal findings of chest CT

Imaging finding	First CT (n = 66)	Second CT (n = 66)
Cardiomegaly	6 (9.1)	6 (9.1)
Atherosclerotic plaque	23 (34.8)	22 (33.3)
Pleural effusion	1 (1.5)	13 (19.7)
Pericardial effusion	-	1 (1.5)

Data are reported as n (%). CT: Computed tomography.

Several factors, including patient's age, duration of hospitalization, presence of comorbidities, and severity of lung disease, have been proposed to determine the risk of residual lung abnormalities among survivors of viral pulmonary infections [21], [26], [27]. The mean age of patients in our study was 56 years; previous studies have shown that OP usually presents within the fifth and sixth decades of life [28]. In this study, patients had a 10-day hospital length of stay, similar to previous reports [29], [30]. In addition, 27% and 35% of the patients had diabetes and hypertension, respectively, which is higher than the prevalence of diabetes and hypertension among the general population with COVID-19 [31], [32], [33]. Follow-up studies are needed to verify whether these factors contribute significantly to the development of residual fibrosis in patients with COVID-19.

Our results showed that after approximately 8 days, GGO, the main imaging finding on initial CT, had been replaced by viral-induced lung damage (OP-like pattern). The axial distribution of pulmonary lesions did not change between the initial and second CT scans; the majority of lesions had a peripheral distribution, in line with previous reports in patients with COVID-19 [1]. Along with viral-induced lung damage (OP-like pattern), sub-pleural band, bronchial dilation, and reticulation were the most common patterns observed on second CT scans and were predominantly observed in the lower lobes. These patterns that may be a manifestation of OP-associated fibrosis have been reported to be predominantly lower-lobe dependent in other studies [34], [35]. In patients with SARS, reticular changes were observed nearly 2 weeks after the onset of initial symptoms and remained stable after 4 weeks in more than half of the patients. Bronchial dilation was also evident in a few patients after the 4th week [36]. Our study showed that in patients who had undergone a third CT scan, reticulation was more commonly observed compared with previous CT scans. Furthermore, the observation of these patterns on chest CT, as well as other findings such as reversed-halo sign can provide a clue about the stage of the disease and guide physicians to select the most appropriate treatment strategy that is most beneficial in the post-acute phase of the disease. This will help in optimizing resource allocation and avoiding unnecessary acute-phase treatments to patients.

Based on our results, while pleural effusion was only evident in one initial CT, 13 patients had pleural effusion on the second CT. In a systematic review, Salehi *et al*. found that pleural effusion is one of the less common imaging findings associated with COVID-19 that may be seen with disease progression [1]. Of the four patients in our study who experienced death, three patients had atherosclerotic plaques on imaging, and two had concomitant cardiomegaly and pleural effusion.

In terms of management of patients with the secondary OP, the treatment of OP mainly consists of corticosteroid therapy, as well as treating the underlying disease [17], [28]. Most recently, preliminary results

from the RECOVERY trial showed that dexamethasone has the potential to reduce mortality by 30% in critically ill patients with COVID-19 [37]. This could be due to the effect of corticosteroids on the degradation of fibroblastic plugs in those patients with OP pattern on chest imaging, thereby reducing mortality.

Conclusion

In this study, we showed that the total CT scores of patients with COVID-19 who developed an OP –like pattern on CT imaging during hospitalization had a steady rise from 1st day of admission to approximately 17 days later, and the right lower lobe had the highest involvement at all-time points. In addition, observation of imaging findings such as the reversed halo sign, which indicates that the viral response phase has already occurred, should prompt physicians to use medications other than antivirals since they are less likely to provide any benefits to the patient in the later phases of disease. Taken together, serial CT imaging renders helpful information that could be implemented in the management of patients with COVID-19.

Acknowledgments

We would like to acknowledge all healthcare workers who passed away during the COVID-19 pandemic, particularly our co-author, Prof. Shahram Kahkouee, who sadly passed away on December 21, 2020.

References

1. Salehi S, Abedi A, Balakrishnan S, Gholamrezanezhad A. Coronavirus disease 2019 (COVID-19): A systematic review of imaging findings in 919 patients. Am J Roentgenol. 2020;215(1):87-93. https://doi.org/10.2214/ajr.20.23034
   PMid:32174129
2. Ng MY, Lee EY, Yang J, Yang F, Li X, Wang H, *et al*. Imaging profile of the COVID-19 infection: Radiologic findings and literature review. Radiol Cardiothorac Imaging. 2020;2(1):e200034. https://doi.org/10.1148/ryct.2020200034
3. Long C, Xu H, Shen Q, Zhang X, Fan B, Wang C, *et al*. Diagnosis of the Coronavirus disease (COVID-19): rRT-PCR or CT? Eur J Radiol. 2020;126:108961. https://doi.org/10.1016/j.ejrad.2020.108961
   PMid:32229322
4. Zhang P, Li J, Liu H, Han N, Ju J, Kou Y, *et al*. Long-term bone and lung consequences associated with hospital-acquired severe acute respiratory syndrome: A 15-year follow-up from a prospective cohort study. Bone Res. 2020;8:8. https://doi.org/10.1038/s41413-020-00113-1
   PMid:32128276
5. Walsh SL, Hansell DM. Diffuse interstitial lung disease: Overlaps and uncertainties. Eur Radiol. 2010;20(8):1859-67. https://doi.org/10.1007/s00330-010-1737-3
   PMid:20204644
6. Lai R, Feng X, Gu Y, Lai HW, Liu F, Tian Y, *et al*. Pathological changes of lungs in patients with severity acute respiratory syndrome. J Zhonghua Bing Li Xue Za Zhi. 2004;33(4):354-7.
   PMid:15363323
7. Ajlan AM, Ahyad RA, Jamjoom LG, Alharthy A, Madani TA. Middle East respiratory syndrome coronavirus (MERS-CoV) infection: Chest CT findings. Am J Roentgenol. 2014;203(4):782-7. https://doi.org/10.2214/ajr.14.13021
   PMid:24918624
8. Gómez-Gómez A, Martínez-Martínez R, Gotway MB. Organizing pneumonia associated with swine-origin influenza A H1N1 2009 viral infection. Am J Roentgenol. 2011;196(1):W103-4. https://doi.org/10.2214/ajr.10.4689
   PMid:21178022
9. Wu Y, Xie Y, Wang X. Longitudinal CT findings in COVID-19 pneumonia: Case presenting organizing pneumonia pattern. Radiol Cardiothorac Imaging. 2020;2(1):e200031. https://doi.org/10.1148/ryct.2020200031
10. Poggiali E, Dacrema A, Bastoni D, Tinelli V, Demichele E, Ramos PM, *et al*. Can lung US help critical care clinicians in the early diagnosis of novel coronavirus (COVID-19) pneumonia? Radiology. 2020;295(3):E6. https://doi.org/10.1148/radiol.2020200847
    PMid:32167853
11. Maldonado F, Daniels CE, Hoffman EA, Eunhee SY, Ryu JH. Focal organizing pneumonia on surgical lung biopsy: Causes, clinicoradiologic features, and outcomes. Chest. 2007;132(5):1579-83. https://doi.org/10.1378/chest.132.4_meetingabstracts.584c
    PMid:17890462
12. Travis WD, Costabel U, Hansell DM, King TE Jr., Lynch DA, Nicholson AG, *et al*. An official American thoracic society/European respiratory society statement: Update of the international multidisciplinary classification of the idiopathic interstitial pneumonias. Am J Respir Crit Care Med. 2013;188(6):733-48. https://doi.org/10.1164/ajrccm.165.2.ats01
    PMid:24032382
13. Hansell DM, Bankier AA, MacMahon H, McLoud TC, Müller NL, Remy J. Fleischner society: Glossary of terms for thoracic imaging. Radiology. 2008;246(3):697-722. https://doi.org/10.1148/radiol.2462070712
    PMid:18195376
14. Wang D, Hu B, Hu C, Zhu F, Liu X, Zhang J, *et al*. Clinical characteristics of 138 hospitalized patients with 2019 novel coronavirus-infected pneumonia in Wuhan, China. JAMA. 2020;323(11):1061-9. https://doi.org/10.1001/jama.2020.1585
    PMid:32031570
15. Bernheim A, Mei X, Huang M, Yang Y, Fayad ZA, Zhang N, *et al*. Chest CT findings in coronavirus disease-19 (COVID-19): Relationship to duration of infection. Radiology. 2020;295(3):200463. https://doi.org/10.1148/radiol.2020200463
16. Ujita M, Renzoni EA, Veeraraghavan S, Wells AU, Hansell DM. Organizing pneumonia: Perilobular pattern at thin-section CT. Radiology. 2004;232(3):757-61. https://doi.org/10.1148/radiol.2323031059
    PMid:15229349
17. Kligerman SJ, Franks TJ, Galvin JR. From the radiologic pathology archives: Organization and fibrosis as a response to

lung injury in diffuse alveolar damage, organizing pneumonia, and acute fibrinous and organizing pneumonia. Radiographics. 2013;33(7):1951-75. https://doi.org/10.1148/rg.337130057
PMid:24224590

18. Kim H. Outbreak of novel coronavirus (COVID-19): What is the role of radiologists? Eur Radiol. 2020;30(6):3266-7. https://doi.org/10.1007/s00330-020-06748-2
PMid:32072255

19. Salehi S, Reddy S, Gholamrezanezhad A. Long-term pulmonary consequences of coronavirus disease 2019 (COVID-19): What we know and what to expect. J Thorac Imaging. 2020;35(4):W87-9. https://doi.org/10.1097/rti.0000000000000534
PMid:32404798

20. Song F, Shi N, Shan F, Zhang Z, Shen J, Lu H, *et al*. Emerging 2019 novel coronavirus (2019-nCoV) pneumonia. Radiology. 2020;295(1):210-7. https://doi.org/10.1148/radiol.2020200274
PMid:32027573

21. Xie L, Liu Y, Xiao Y, Tian Q, Fan B, Zhao H, *et al*. Follow-up study on pulmonary function and lung radiographic changes in rehabilitating severe acute respiratory syndrome patients after discharge. Chest. 2005;127(6):2119-24. https://doi.org/10.1378/chest.127.6.2119
PMid:15947329

22. Wu X, Dong D, Ma D. Thin-section computed tomography manifestations during convalescence and long-term follow-up of patients with severe acute respiratory syndrome (SARS). Med Sci Monit. 2016;22:2793-9. https://doi.org/10.12659/msm.896985
PMid:27501327

23. Liu D, Zhang W, Pan F, Li L, Yang L, Zheng D, *et al*. The pulmonary sequalae in discharged patients with COVID-19: A short-term observational study. Respir Res. 2020;21(1):125. https://doi.org/10.1186/s12931-020-01385-1
PMid:32448391

24. Pan F, Ye T, Sun P, Gui S, Liang B, Li L, *et al*. Time course of lung changes at chest CT during recovery from coronavirus disease 2019 (COVID-19). Radiology. 2020;295(3):715-21. https://doi.org/10.1148/radiol.2020200370
PMid:32053470

25. Duan YN, Qin J. Pre-and posttreatment chest CT findings: 2019 novel coronavirus (2019-nCoV) pneumonia. Radiology. 2020;295(1):21. https://doi.org/10.1148/radiol.2020200323
PMid:32049602

26. Antonio GE, Wong KT, Hui DS, Wu A, Lee N, Yuen EH, *et al*. Thin-section CT in patients with severe acute respiratory syndrome following hospital discharge: Preliminary experience. Radiology. 2003;228(3):810-5. https://doi.org/10.1148/radiol.2283030726

27. Ong KC, Ng AW, Lee LS, Kaw G, Kwek SK, Leow MK, *et al*. 1-year pulmonary function and health status in survivors of severe acute respiratory syndrome. Chest. 2005;128(3):1393-400. https://doi.org/10.1378/chest.128.3.1393
PMid:16162734

28. Drakopanagiotakis F, Paschalaki K, Abu-Hijleh M, Aswad B, Karagianidis N, Kastanakis E, *et al*. Cryptogenic and secondary organizing pneumonia: Clinical presentation, radiographic findings, treatment response, and prognosis. Chest. 2011;139(4):893-900. https://doi.org/10.1378/chest.10-0883
PMid:20724743

29. Zhou F, Yu T, Du R, Fan G, Liu Y, Liu Z, *et al*. Clinical course and risk factors for mortality of adult inpatients with COVID-19 in Wuhan, China: A retrospective cohort study. Lancet. 2020;395(10229):1054-62. https://doi.org/10.1016/s0140-6736(20)30566-3
PMid:32171076

30. Qiu H, Wu J, Hong L, Luo Y, Song Q, Chen D. Clinical and epidemiological features of 36 children with coronavirus disease 2019 (COVID-19) in Zhejiang, China: An observational cohort study. Lancet Infect Dis. 2020;20(6):689-96. https://doi.org/10.1016/s1473-3099(20)30198-5

31. Fadini GP, Morieri ML, Longato E, Avogaro A. Prevalence and impact of diabetes among people infected with SARS-CoV-2. J Endocrinol Invest. 2020;43(6):867-9. https://doi.org/10.1007/s40618-020-01236-2
PMid:32222956

32. Wang X, Wang S, Sun L, Qin G. Prevalence of diabetes mellitus in 2019 novel coronavirus: A meta-analysis. Diabetes Res Clin Pract. 2020;164:108200. https://doi.org/10.1016/j.diabres.2020.108200
PMid:32407746

33. Zhu L, She ZG, Cheng X, Qin JJ, Zhang XJ, Cai J, *et al*. Association of blood glucose control and outcomes in patients with COVID-19 and pre-existing Type 2 diabetes. Cell Metabolism. 2020;31(6):1068-77.e3. https://doi.org/10.1016/j.cmet.2020.04.021

34. Kligerman SJ, Groshong S, Brown KK, Lynch DA. Nonspecific interstitial pneumonia: Radiologic, clinical, and pathologic considerations. Radiographics. 2009;29(1):73-87. https://doi.org/10.1148/rg.291085096

35. Lee JW, Lee KS, Lee HY, Chung MP, Yi CA, Kim TS, *et al*. Cryptogenic organizing pneumonia: Serial high-resolution CT findings in 22 patients. AJR Am J Roentgenol. 2010;195(4):916-22. https://doi.org/10.2214/ajr.09.3940
PMid:20858818

36. Ooi GC, Khong PL, Müller NL, Yiu WC, Zhou LJ, Ho JC, *et al*. Severe acute respiratory syndrome: Temporal lung changes at thin-section CT in 30 patients. Radiology. 2004;230(3):836-44. https://doi.org/10.1148/radiol.2303030853
PMid:14990845

37. Randomised Evaluation of COVID-19 Therapy (RECOVERY). Available from: https://www.clinicaltrials.gov/ct2/show/NCT04381936. [Last accessed on 2020 Jun 18].